Chem. Senses 26: 399–407, 2001

Slice Culture of the Olfactory Bulb of *Xenopus laevis* Tadpoles

Uwe Scheidweiler, Leonid Nezlin, Jörg Rabba, Birgitt Müller and Detlev Schild

Physiologisches Institut, Universität Göttingen, Humboldtallee 23, D-37073 Göttingen, Germany

Correspondence to be sent to: Detlev Schild, Physiologisches Institut, Universität Göttingen, Humboldtallee 23, D-37073 Göttingen, Germany. e-mail: dschild@gwdg.de

Abstract

We report on the development of a slice culture of amphibian brain tissue. In particular, we cultured slices from *Xenopus laevis* tadpoles that contain the olfactory mucosae, the olfactory nerves, the olfactory bulb and the telencephalon. During 6 days in roller tubes the slices flattened, starting from 250 μm and decreasing to ~40 μm, corresponding to about three cell layers. Dendritic processes could be followed over distances as long as 200 μm. Neurons in the cultured slice could be recorded using the patch clamp technique and simultaneously imaged using an inverted laser scanning microscope. We characterized the main neuron types of the olfactory bulb, i.e. mitral cells and granule cells, by correlating their typical morphological features in the acute slice with the electrophysiological properties in both the acute slice and slice culture. This correlation allowed unambiguous identification of mitral cells and granule cells in the slice culture.

Introduction

Over the last decade we have made considerable progress in understanding the olfactory system. A large number of olfactory receptors have been characterized in several species (Buck and Axel, 1991; Ngai *et al.*, 1993; Raming *et al.*, 1993; Dulac and Axel, 1995; Freitag *et al.*, 1995; Nekrasova *et al.*, 1996; Weth *et al.*, 1996; Wellerdieck *et al.*, 1997; Berghard and Dryer, 1998) and olfactory receptor neurons have been shown to project in a specificity-guided way onto the olfactory bulb (OB) (Mombaerts, 1996), where they make synaptic contacts with mitral and periglomerular cells within glomeruli.

The subsequent steps of olfactory signal processing taking place in the OB are less clear, though the complex synaptic interactions between mitral/tufted cells and interneurons as well as their modulation by efferent systems have partly been unraveled using cell culture (Trombley, 1992; Trombley and Shepherd, 1992; Trombley and Westbrook, 1992; Bischofberger and Schild, 1995; Schoppa and Westbrook, 1997) and slice preparations from rat (Chen and Shepherd, 1997; Isaacson and Strowbridge, 1998; Halabisky *et al.*, 2000) and frog (Bardoni *et al.*, 1996). In cell culture mitral cells (MCs) lack afferent physiological input as well as their output targets and might make non-physiological synaptic contacts. As to the OB slice, the three-dimensional cytoarchitecture of the OB is not as well suited to sectioning as that of the hippocampus or cerebellum. Many of the long processes of MCs and granule cells (GCs) are necessarily injured and partly lost during sectioning. Another disadvantage of thick slices is the poor transparency, so that in the case of simultaneous patch clamping and imaging, upright optics with relatively small apertures have to be used. In conventional microscopy this means a loss of resolution and light transmission efficiency.

Taken together, each preparation for studying OB neurons has major drawbacks, which is presumably one of the reasons why the cellular physiology of the hippocampus and cerebellum have been studied in considerably more detail than that of the OB.

In this paper we propose slice culture of the tadpole OB as a novel *in vitro* preparation for studying OB neurons. This preparation has the advantages that: (i) the amount of damage caused by sectioning the brain tissue is limited; (ii) the slice is connected to the olfactory mucosa and retains connections to higher olfactory centers; (iii) synaptic connectivity appears to be intact; (iv) the thickness of the slice (40–50 μm) allows simultaneous imaging and patch clamp experiments.

We demonstrate the basic morphological and electrophysiological properties of the slice culture and characterize the two main neuron types of the OB slice culture by comparing them with the corresponding neuron types in an acute OB slice.

Materials and methods

Acute slices

Tadpoles of *Xenopus laevis* (stages 52–54) (Nieuwkoop and Faber, 1956) were anaesthetized and immobilized in a mixture of ice and water. A block of tissue containing the mucosa, the olfactory nerves and the anterior two thirds of

the brain were cut out, glued on the stage of a vibroslicer (VT 1000; Leica, Bensheim, Germany) and cut horizontally into 250 μm thick slices. The slices were placed under a harp-like grid in a recording chamber and viewed using an upright microscope equipped with DIC optics (Axioskop 2; Zeiss). In the vibratome chamber and in the experimental chamber the slices were covered by bath solution (see Solutions). MCs and GCs were chosen according to the layering of the OB.

To visualize cell processes, 0.5% biocytin (Molecular Probes) was added to the pipette solution. After the experiment cells were filled using a depolarizing current (2 s pulses at 0.25 Hz for 5–10 min). The preparations were left in fresh saline for 20–30 min and fixed in 4% paraformaldehyde (PFA) in 0.1 M phosphate buffer, pH 7.4, (PB) at 4°C, rinsed in PB, left overnight in PB with 0.5% Triton X-100 (TX) and then immersed in a solution of avidin, Alexa Fluor 488 conjugate (5 μg/ml in PB with TX; Molecular Probes) for 4–6 h at room temperature. The specimens were rinsed several times in PB, embedded in PB containing glycerol (1:1) and examined using a laser scanning confocal microscope (Zeiss LSM 510). A number of optical sections, indicated for each figure, were projected onto one image (LSM 510 software) and the layout of the figures was done using Adobe Photoshop. The images are always shown as negatives.

Slice cultures

Xenopus laevis tadpoles of stages 52 and 53 were taken from the rearing tank and put into a bath of $KMnO_4$ (7.5 μM) for 15 min. They were then anaesthetized in a mixture of ice and water, washed for a few seconds in non-methylated ethanol (70%) and rinsed in sterile bath solution. The anaesthetized tadpoles were decapitated under a dissection microscope and a tissue block containing the mucosae, the olfactory nerves and the forebrain was cut out. Using a vibratome (VT1000) we sectioned the tissue block into three slices, the second of which contained the olfactory mucosae, the olfactory nerves and the OBs. When the OB was to be cultured alone, mucosae, nerves and surrounding tissue were removed under a dissection microscope. The slices were then transferred to roller tubes (see below).

The embedding and culturing procedures were similar to those described by Gähwiler (Gähwiler, 1981, 1988; Gähwiler *et al.*, 1997). Briefly, drops (30 μl each) of reconstituted lyophilized chicken plasma (0.2 mg% heparin; Cocalico Biologicals, Reamstown, PA) were put on 12 × 24 mm^2 sterile coverslips (Kindler, Freiburg im Breisgau, Germany). The osmolarity of the plasma was adjusted to 230 mOsm. Using a small spatula, each slice was carefully transferred to a drop of plasma, which was then spread out to cover most of the coverslip. We then added 30 μl of thrombin (Merck, Darmstadt, Germany) the activity of which had been reduced to 167 U/ml by adding sterile solution B. Plasma and thrombin were thoroughly mixed to support clotting. Finally, the slice was placed in the center of the coverslip.

The plated slices were immediately transferred to roller tubes (Nunclon delta tubes, catalog no. 156758; Nunc, Denmark) filled with 750 μl of HEPES-buffered amphibian cell culture medium (FM-65-L; C.C.Pro, Neustadt/W, Germany) containing 5% equine serum (Gibco) and 5 mg% gentamicin (Sigma). The osmolarity of the medium was adjusted to 225 mOsm with tissue culture water (Sigma).

The Nunclon culture tubes were placed in the holes of a rotating disk (360 r.p.m.) housing 24 tubes. The disk was tilted by 10° with respect to the vertical and moved by a stepper motor (escap; API Portescap, Pforzheim, Germany), which was driven by a microcontroller (Schild *et al.*, 1996) and custom-made hardware. The slices were cultured at room temperature (20–22°C) under normal ambient conditions. The culture medium was exchanged every 4–6 days.

To monitor the development of the slice culture, we stained 356 slices after a variable number of days in culture using either fluorescein diacetate or propidium iodide (10 μg/ml). The slices were fixed in PFA, washed in PB and embedded in PB with glycerol. In particular, we checked the overall structure of the slice, the organization of cell layers and the thickness of the slice. The images are shown as negatives.

Prior to recording from a cultured slice it was detached from the coverslip and transferred to the recording chamber under solution B. Plasma clots were carefully removed and the slice was fixed in the recording chamber under a harp-like grid.

Patch clamp recordings

The experiments were carried out at room temperature. Acute slices were placed under an upright microscope (Axioskop 2) whereas cultured slices were recorded on the stage of an inverted microscope (Axiovert 100TV; Zeiss) to which the head stage of a patch clamp amplifier and a laser scanning microscope (LSM 510; Zeiss) were attached. Electrodes with a tip diameter of 1–2 μm and a resistance of ~7 MΩ were fabricated from borosilicate glass (1.8 mm outer diameter; Hilgenberg, Malsfeld, Germany) using a two-stage electrode puller (Narishige, Tokyo, Japan). The pipettes were fire polished. Pulse protocols, data acquisition and evaluation programs were written in C. Pulses were delivered from a microcontroller (Schild *et al.*, 1996) to a D/A converter and then to the patch clamp amplifier (EPC7; List, Darmstadt, Germany). Currents and voltages were recorded on video tapes using a pulse code modulation unit (Instrutech, Elmont, NY). The data were digitized off-line using an 8 pole Bessel filter, an A/D converter and a PC. Further data analysis was performed under LINUX or WINDOWS.

Solutions

The following solutions were used. Bath solution (B): 98 mM NaCl, 2 mM KCl, 1 mM $CaCl_2$, 2 mM $MgCl_2$, 5 mM glucose, 5 mM sodium pyruvate, 10 mM HEPES. Pipette solution: 2 mM NaCl, 11 mM KCl, 2 mM $MgSO_4$, 80 mM potassium gluconate, 10 mM HEPES, 0.2 mM EGTA, 1 mM Na_2-ATP, 0.1 mM Na_2-GTP. All solutions were at pH 7.8 (Howell *et al.*, 1970). The osmolarities of the bath and pipette solutions were adjusted to 225 and 190 mOsm, respectively. The bath solution was applied by gravity feed from storage syringes through a funnel drug applicator (Schild, 1985) to the recording chamber. The flow was 250 µl/min. Chemicals were purchased from Sigma, Merck and Calbiochem (La Jolla, CA).

Where indicated, sodium channels were blocked by TTX (1 µM) (Sigma) dissolved in the bath solution. In some experiments Fluo3 (25 µM) and FuraRed (75 µM), both obtained from Molecular Probes (Leiden, The Netherlands), were added to the pipette solution.

Results

The morphology of a typical acute slice is shown in Figure 1A,B. Figure 1A shows an overview of the olfactory mucosae, the olfactory nerves, the OB and the telencephalon. The acute slices of the OB were ~250 µm thick and contained ~25 cell layers (Figure 2, d1).

During the first 6 days in the roller wheel the overall aspect of the slice appeared largely unchanged (Figure 1C),

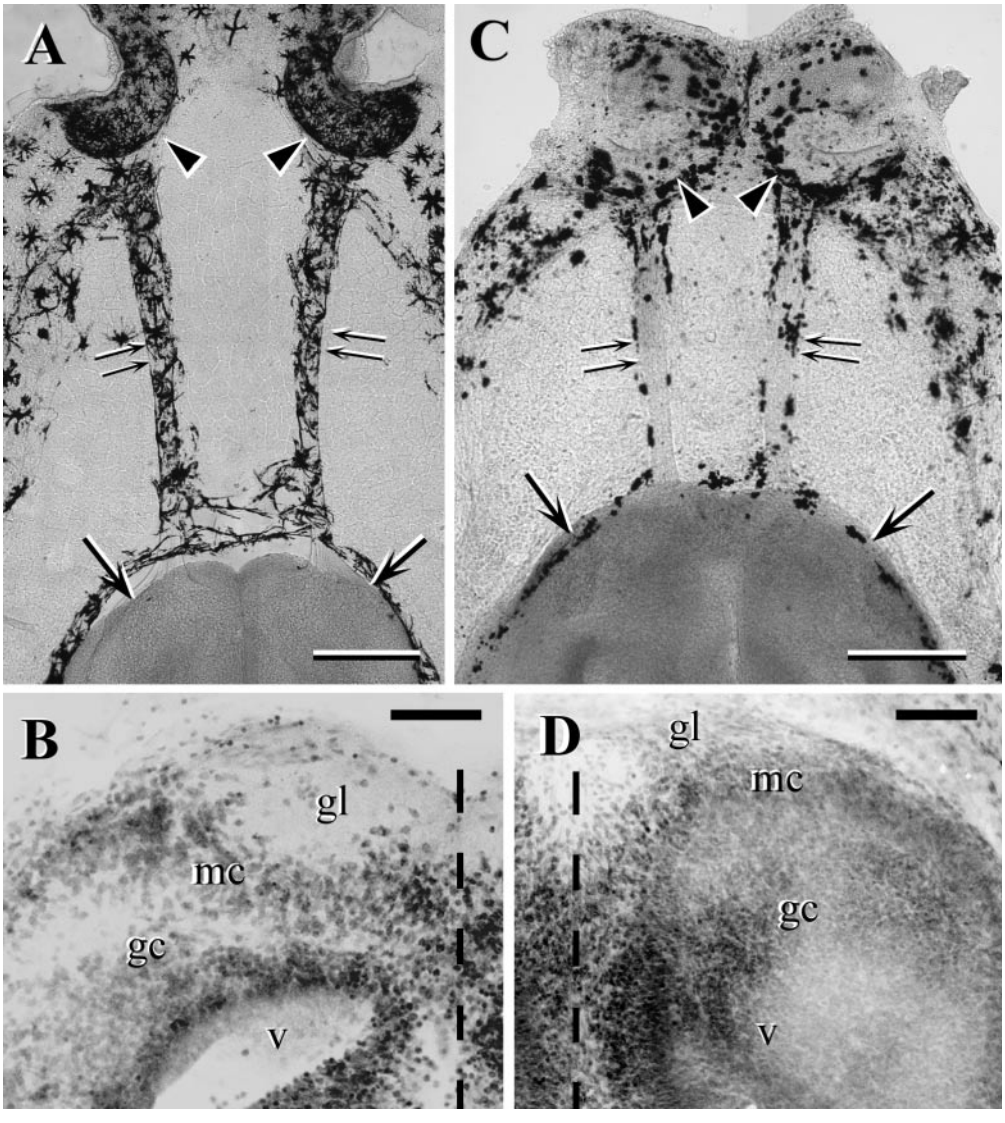

Figure 1 Comparison of the acute OB slice with the cultured slice. **(A)** Overview of a 250 µm thick acute slice containing right and left OB (arrows), olfactory nerves (double arrows) and olfactory mucosae (arrowheads). Mucosae and nerves are partly covered by melanocytes. **(B)** Acute slice of the forebrain (250 µm thick, left half) stained with propidium iodide. gc, granule cell layer; gl, glomerular layer; mc, mitral cell layer; v, ventricle; dotted line, the midline of the brain. **(C)** A cultured slice after 6 days *in vitro*. Mucosae, nerves and bulb marked as in (A). **(D)** Slice of the forebrain after 6 days in culture [stained as in (B), right half]. Abbreviations as in (B). Scale bars: (A,C) 500 µm; (B,D) 100 µm.

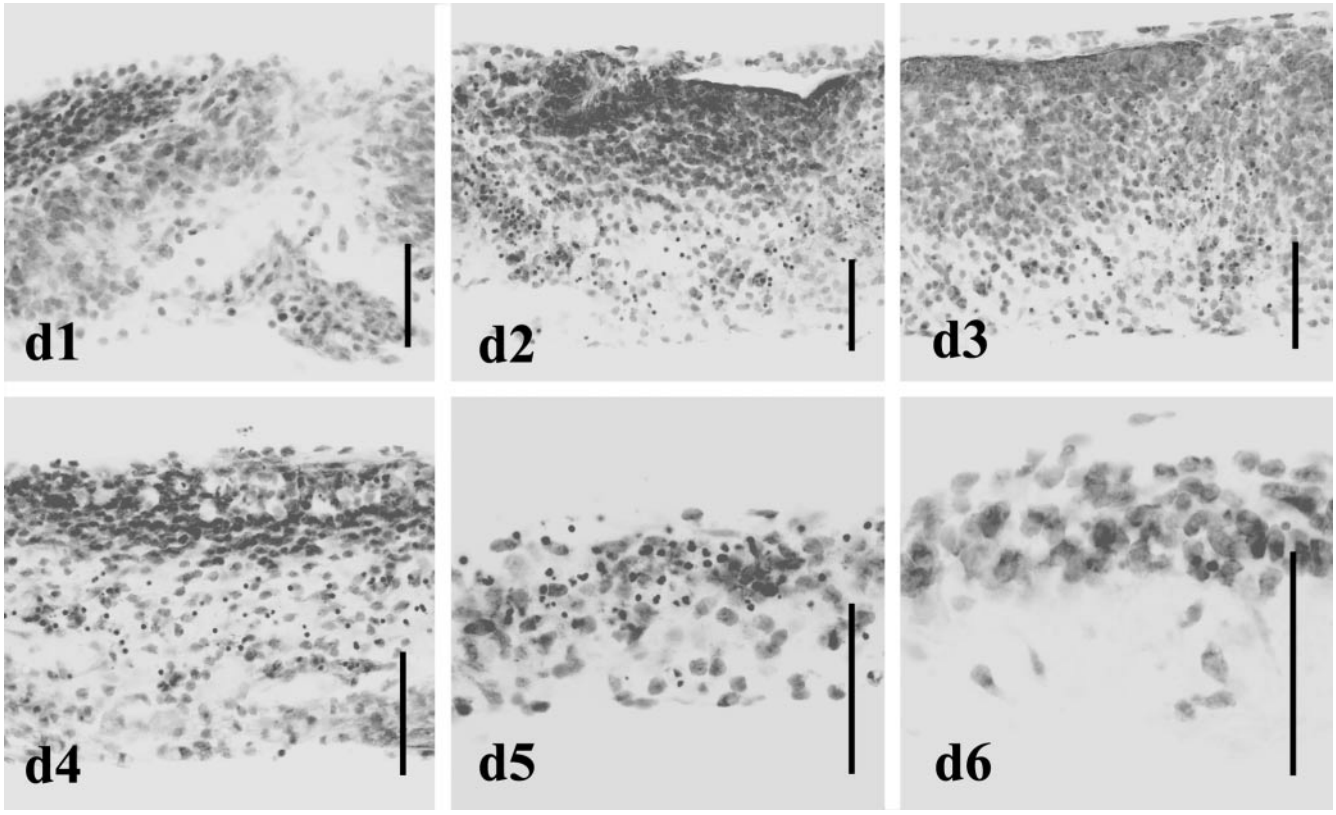

Figure 2 Coronal sections of cultured slices from day 1 (d1) to day 6 (d6). Note the gradual decrease in cell layers from ~25 to ~3 layers at day 6. Slices were stained with propidium iodide and imaged using a laser scanning confocal microscope. Scale bars: 100 μm.

although it had undergone the following characteristic changes. The mucosae were slightly flattened and the general cytoarchitecture and layering were less distinct than in the acute slice (Figure 1D versus B). The ventricles could be clearly recognized, although their free lumen was narrowed.

Over 5 days in culture the slices flattened (Figure 2) and on day 6 *in vitro* they contained about three (3 ± 1) cell layers (Figure 2, d6). The slices could then be recorded from and simultaneously imaged using inverted optics. Figure 3 shows a neuron of the OB that was patch clamped and filled with the calcium indicator dye FuraRed through the pipette. The cell processes could be followed over long distances.

The cytoarchitecture of the *Xenopus* OB (Figure 1B) is not as neatly layered as it is in many mammals and the cytoarchitecture of the slice culture appears even less ordered (Figure 1D). We therefore established on-line criteria for identifying the main cell types following three steps. In step 1 we recorded from the cells of the cultured OB and grouped the cells according to simple electrophysiological criteria. In step 2 we did the same in acute OB slices and stained the cells with biocytin/avidin (see Materials and methods). In step 3 we correlated the morphological characteristics of the cells with the electrophysiological properties of the two main neuron types.

In the voltage clamp type A neurons showed a fast inward current and a deactivating outward current (Figure 4A). The

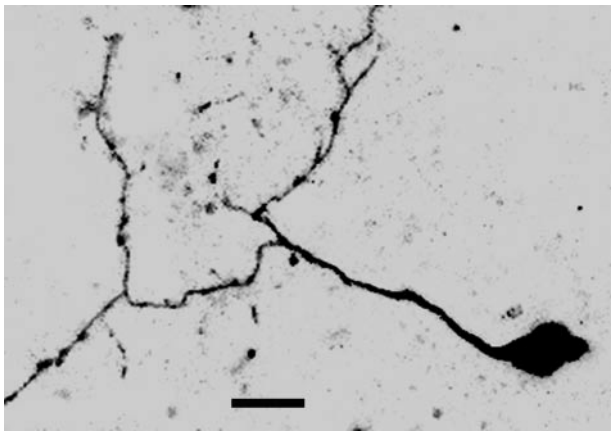

Figure 3 Laser scanning confocal microscope image of a neuron filled with Fura Red (75 μM) in a cultured slice at day 6. Optical slices: 3 × 2.8 μm. Scale bar: 10 μm.

steady-state I–V curve of the outward current showed peak amplitudes at ~20 mV (Figure 4B), suggesting the presence of a Ca^{2+}-dependent K^+ current (Heyer and Lux, 1976; Hille, 1992).

The fast inward current, seen as a short negative peak at the onset of the response of the voltage clamp pulse (Figure 4A), is represented at higher resolution in Figure 4C. It

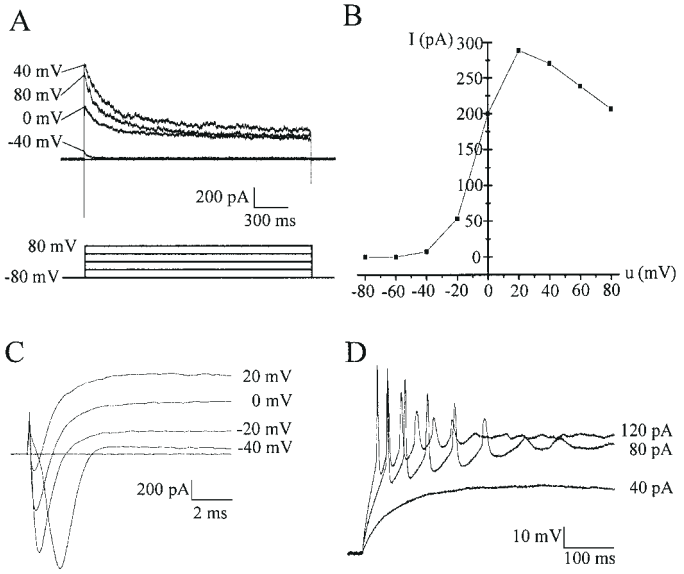

Figure 4 Whole cell recordings from a type A neuron after 6 days in culture. **(A)** Current responses to voltage pulses from –80 to 80 mV in 20 mV steps. For clarity, only the steps to –40, 0, 40 and 80 mV are shown in this part of the figure. Fast inward current and slowly deactivating outward current. **(B)** *I–V* curve of steady-state outward currents obtained from the response to pulses at 20 mV steps and averaged over the last 50 ms of a 2 s pulse, respectively. **(C)** Fast inward current shown in (A) at a higher time resolution. **(D)** Sub-threshold and supra-threshold voltage responses to current injections show passive depolarization and spike trains with decreasing amplitudes.

activated at about –50 mV and was TTX sensitive (not shown). The input impedance at –80 mV was 2.27 ± 0.23 GΩ (mean ± SEM, 15 cells). Current injections elicited spikes, the amplitudes of which decreased, presumably due to inactivation of sodium and fast potassium channels. The membrane time constant was ~50 ms (11 cells).

Neuron type B showed quite a different behavior. Upon depolarization in the voltage clamp fast and TTX-sensitive inward currents were observed which activated with a delay after the onset of the voltage pulse (Figure 5A). They were repetitive and never occurred at the onset of a pulse. The delay decreased with more depolarized potentials. Typically, every inward current was followed by a small and transient outward current (Figure 5A, middle trace). This combination of inward and outward currents is characteristic of action potential (AP)-associated currents (APacs). The APs were presumably generated in an electrotonically peripheral compartment of the neuron which was not voltage clamped.

A comparison of a spike in the current clamp to an APac in the voltage clamp (Figure 5C) supports this interpretation.

When the cell was clamped to increasing steps of injected current the first action potential usually occurred after a long delay of up to 500 ms (Figure 5B). With increasing amplitudes of injected current the delay shortened. The average input impedance of this cell type was 2.18 ± 0.1 GΩ (15 cells).

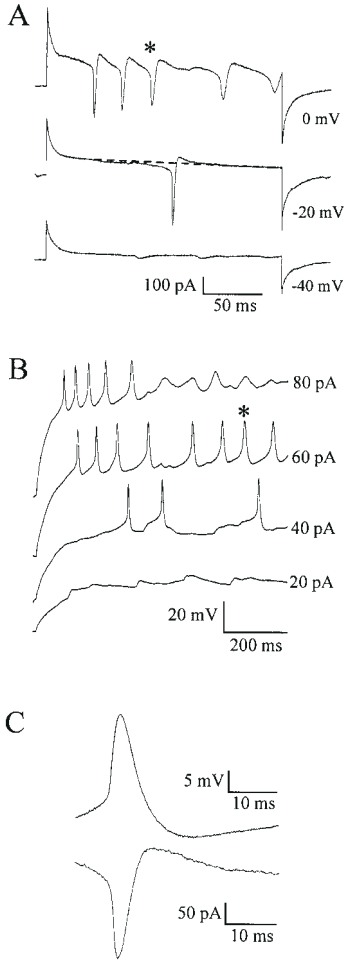

Figure 5 Whole cell recordings from a type B neuron after 6 days in culture. **(A)** Current responses to voltage pulses (holding potential –80 mV) show a delayed fast inward current followed by a small transient outward current (middle trace, dotted line). With increasing voltage the transient inward currents occurred as a train. **(B)** Voltage responses to injection of stepwise increasing current pulses. The trace for the 40 pA injected current is characteristic of this neuron type. Subsequent to a fast initial depolarization the depolarization slows down prior to spike generation. This effect is less prominent at larger injected currents. **(C)** Comparison of an action potential (upper trace, current clamp) with the typical sequence of delayed inward current and small transient outward current (lower trace, voltage clamp). These traces were taken from (B) and (A), respectively, where indicated by asterisks.

Recordings in the acute OB slice showed the same cell types as found in the cultured slice, whereby type A neurons were found in the GC layer, while type B were located in the MC layer (Figures 1B, 7A).

The early inward current and the spiking behavior of type A cells in the acute slice are shown in Figure 6A,B, while the delayed APac and the delayed AP generation of type B cells are shown in Figure 6C,D.

To correlate the electrophysiological response type with neuron morphology we stained the neurons with biocytin/avidin. Type A and type B neurons had the typical branching patterns of GCs (Figure 7B) and MCs (Figure 7C,D),

respectively, and the location of these neurons in the fresh slice unambiguously identified them as GCs and MCs (Figure 7A).

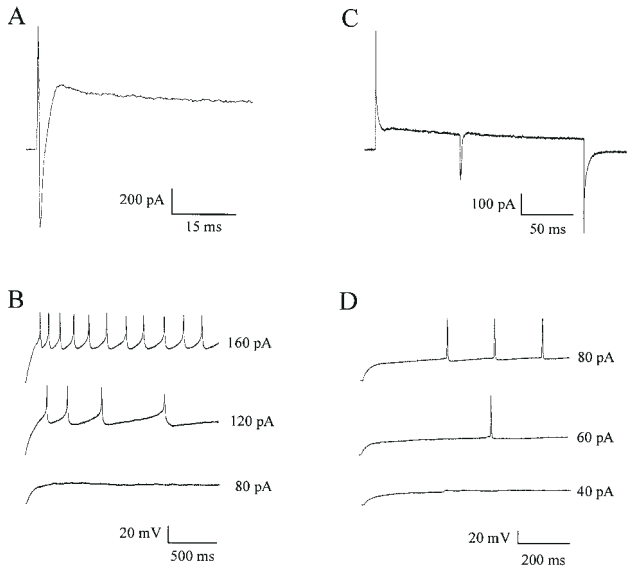

Figure 6 Whole cell recordings from a GC **(A,B)** and a MC **(C,D)** in the acute slice. The morphologies of these cells are represented in Figure 7. **(A)** Fast inward current upon a depolarizing pulse to –40 mV (holding potential –80 mV) recorded in a GC. **(B)** Current clamp recordings from a GC upon injection of a current pulse. **(C)** MC showing a delayed inward current followed by a small transient outward current upon a depolarizing voltage step from –80 to –40 mV. **(D)** In the current clamp spikes of MCs occurred with a delay of up to 500 ms.

The GC (Figure 7B) has one dendrite that travels through the external plexiform/MC layer, while the other dendrites run next to the border of the external plexiform layer. The GC dendrites have a typical thorny appearance (Figure 7B, inset).The MC shown in Figure 7C has several primary and secondary dendrites, the former of which terminate as dendritic tufts (Figure 7D).

These characteristic morphological features were likewise observed in cultured slices.

Figure 8A shows a piece of a GC dendrite with small thorny processes, while Figure 8B,C show the dendritic branching pattern of a neuron with smooth dendrites terminating in dendritic tufts.

Discussion

Olfactory bulb preparations

The electrophysiological behavior of OB neurons has been studied with sharp electrodes *in vivo*, in whole mount and in half bulb preparations, as well as by patch clamp methods in cultured OB neurons and OB tissue slices. Most of the work with sharp electrodes has been reviewed by Mori (Mori, 1987).

Cell cultures were used to study glutamergic transmission from MCs to GCs and its modulation by norepinephrine (Trombley, 1992; Trombley and Shepherd, 1992; Trombley and Westbrook, 1992; Bischofberger and Schild, 1995).

Tissue slices (Edwards *et al.*, 1989) have been used to study glutamergic synaptic transmission within glomeruli

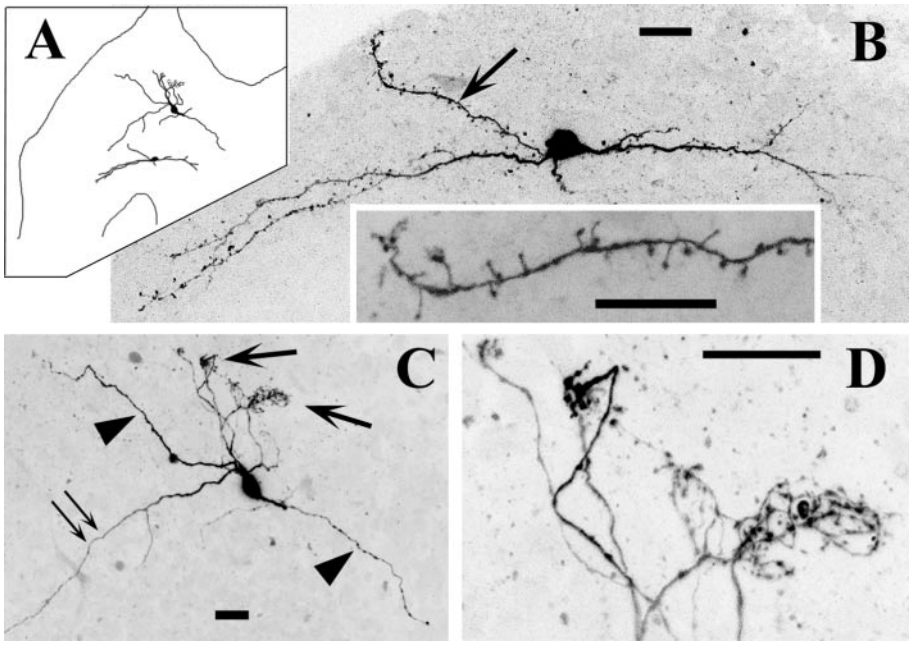

Figure 7 Laser scanning confocal microscope images of a MC and GC in the acute slice (biocytin/avidin staining). The electrophysiological behavior of these cells is shown in Figure 6. **(A)** Schematic drawing of the left OB indicating the position of the cells presented in (B) and (C). **(B)** GC (53 × 0.55 μm). **(Inset)** Higher magnification of the dendrite indicated by the arrow. Note the gemmules issuing from the dendritic shaft (20 × 0.45 μm). **(C)** MC innervating two glomeruli (arrows) and having two additional dendrites (arrowheads) as well as an axon (double arrow) (53 × 0.95 μm). **(D)** Detail of (C). Glomerular tufts at higher magnification (52 × 0.8 μm). Scale bars: 10 μm.

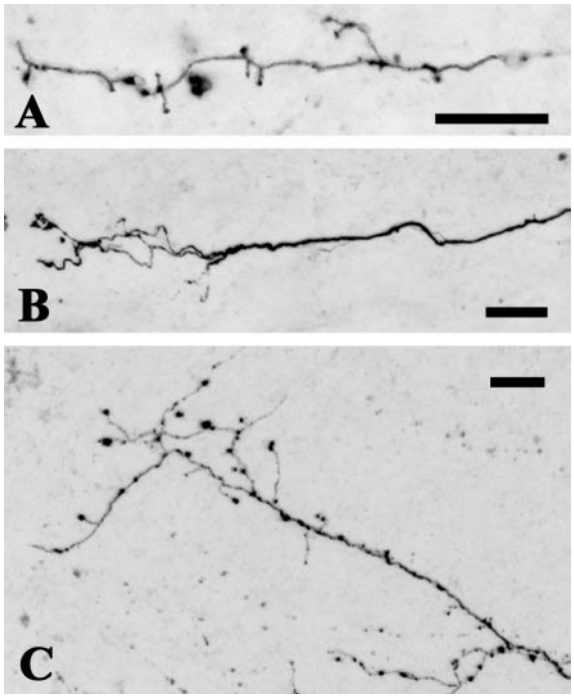

Figure 8 Laser scanning confocal microscope images of biocytin-filled dendrites in type A and type B cells after 7 days in culture. **(A)** Dendrite of a type A neuron bearing gemmules (compare with the inset in Figure 7A) (4 × 0.8 μm). **(B)** Smooth dendrite of a type B neuron (15 × 0.7 μm). **(C)** Another dendrite of the same type B neuron terminating with a dendritic tuft (compare with Figure 7D) (21 × 0.7 μm). Scale bars: 10 μm.

(Bardoni *et al.*, 1996; Chen and Shepherd, 1997; Isaacson, 1999) and at reciprocal synapses (Bardoni *et al.*, 1996; Isaacson and Strowbridge, 1998; Halabisky *et al.*, 2000), action potential back-propagation (Bischofberger and Jonas, 1997), and noradrenergic modulation of synaptic transmission via α_1-receptors (Ciombor *et al.*, 1999) and α_2-receptors (Czesnik *et al.*, 2001).

To obtain the maximum information from OB neurons it would be desirable to make simultaneous patch clamp and imaging recordings. However, due to the complex three-dimensional branching patterns of OB neurons, on the one hand, and the technical limitations of upright optics, on the other, this is extremely difficult in OB slices. To overcome this problem, cultured slices can be used (Gähwiler, 1981; Kanaki *et al.*, 1997), where inverted optics with maximum resolution and high fluorescence intensity allow the study of processes in almost two-dimensional dendritic branching patterns. We have developed a slice culture of *X. laevis* tadpoles where mucosa and bulb can be cultured as one tissue piece. To our knowledge this is the first slice culture of amphibian brain tissue and we show that simultaneous patch clamp and imaging recordings are feasible in this preparation.

Development of the slice culture over time

There are some characteristic differences between the *Xenopus* OB slice culture and rodent slice cultures (Gähwiler, 1981; Gähwiler *et al.*, 1997). The morphological changes in the *Xenopus* OB slice culture occur more rapidly than those in rodent slice cultures. After ~5 days *in vitro* the *Xenopus* OB slices showed an average of 3 ± 1 cell layers. Over these days the slice thickness decreased from ~250 to ~40–50 μm (Figure 2). After day 6 the number of layers as well as the thickness of the slice stayed approximately constant. After 14 days *in vitro* the layers were not homogeneous and there were numerous cell-free patches in the slice. The product of (number of cell layers) × (days *in vitro*) was lowest on day 6. We therefore made recordings between days 5 and 7. In contrast, rodent slices are usually kept *in vitro* for several weeks (Gähwiler, 1981; Gähwiler *et al.*, 1997).

The more rapid processes in tadpole slice cultures are presumably due to the larval stage at which the tissue was explanted and during which neuronal reorganization processes are much faster than in adults. Similarly, fast processes have been reported in slice cultures from rodent embryonic tissue (Gähwiler *et al.*, 1997).

A second difference between the larval *Xenopus* culture and rodent cultures is with regard to the cytoarchitecture of the slices. Rodent slice cultures of hippocampus or cerebellum retain their layered structure amazingly well over a long time. This is less obvious in the *Xenopus* OB slice culture, first because the cytoarchitecture of the amphibian OB is not as neatly stratified as in higher vertebrates (Shepherd, 1972; Byrd and Burd, 1991; Scalia *et al.*, 1991) and changes are less obvious. Second, changes of the cyto-architecture might be more pronounced in larval tissue (Gähwiler *et al.*, 1997). For patch clamp experiments in both acute and cultured amphibian slices an electrophysiological on-line characterization of cell types is therefore absolutely necessary.

A third difference between the cultured mucosa/OB slice on the one hand and brain slices on the other is the fact that the mucosa/OB slice contains, in addition to neural tissue, epithelial and mesenchymal structures. The obvious advantage is that the olfactory mucosa and its nerve are part of the preparation, which may be useful in some respects. The disadvantage is that the extra-nervous tissues appeared to lyse the plasma clot more rapidly than the brain tissue, which sometimes resulted in partial detachment of the slice.

Electrophysiological characteristics of OB neurons

We have found that a simple distinction between OB cell types can be made by observing input resistances and inward current characteristics. Neurons in both the slice and the slice culture were easily distinguished from glia by the low input resistance of glial cells (<400 MΩ). In addition, glia cells showed almost ohmic *I–V* curves and lacked voltage-dependent sodium currents (not shown). The neurons fell into two large classes.

One class showed a delayed inward current and a delayed

spiking behavior in the current clamp. The dendritic branching pattern of cells belonging to this class clearly showed glomerular tufts. Hence, these neurons were categorized as MCs. Lacking morphological and electrophysiological evidence, we were unable to discern a difference between MCs and tufted cells.

Delayed spike generation has been observed in rat MCs (Chen and Shepherd, 1997), where it was explained by an A-type potassium current responsible for the delayed activation of MCs. In tadpole MCs the delayed spiking in the current clamp corresponded to delayed and transient currents in the voltage clamp which cannot be explained by an A-type current. Though we cannot exclude an A-type current in tadpole MCs, we have observed another feature of MCs that would explain the delayed spiking. In some of the MCs stained with biocytin/avidin the axon issued from the proximal dendritic tree rather than from the soma (data not shown), while in other cases the axon could not be identified unambiguously. Spikes might thus be generated in a dendritic compartment of the MC that cannot be voltage clamped. In any case, the delayed spiking was characteristic of neurons with dendritic tufts in the glomerular layer and located in the external plexiform/mitral cell layer. The delayed spiking can thus be taken as a useful criterion for differentiating neuron classes.

The second class of neurons found in the GC layer near the ventricle always showed a classical Hodgkin–Huxley-like sodium current and the according spiking behavior. All of the GCs recorded in both the slice and the slice culture were spiking interneurons. The amplitudes of the sodium current varied between 650 pA and 2.4 nA. In the *Xenopus* tadpole OB slice the few cell bodies of periglomerular cells are located rostrally in the GL far from any GCs or MCs (Nezlin and Schild, 2000), so that periglomerular cells can be identified unambiguously and independently from the above criteria.

Acknowledgements

We are deeply indebted to Prof. Gähwiler and collaborators for having taught us many valuable details of slice culturing. This work was supported by DFG, SFB 406, B5.

References

Bardoni, R., Magherini, P.C. and **Belluzzi, O.** (1996) *Excitatory synapses in the glomerular triad of frog olfactory bulb* in vitro. NeuroReport, 7, 1851–1855.

Berghard, A. and **Dryer, L.** (1998) *A novel family of ancient vertebrate odorant receptors*. J. Neurobiol., 37, 383–392.

Bischofberger, J. and **Jonas, P.** (1997) *Action potential propagation into the presynaptic dendrites of rat mitral cells*. J. Physiol. (Lond.), 504, 359–365.

Bischofberger, J. and **Schild, D.** (1995) *Different spatial patterns of [Ca^{2+}] increase caused by N- and L-type Ca^{2+} channel activation in frog olfactory bulb neurones*. J. Physiol. (Lond.), 487, 305–317.

Buck, L. and **Axel, R.** (1991) *A novel multigene family may encode odorant receptors: a molecular basis for odor recognition*. Cell, 65, 175–187.

Byrd, C.A. and **Burd, G.D.** (1991) *Development of the olfactory bulb in the clawed frog,* Xenopus laevis*: a morphological and quantitative analysis*. J. Comp. Neurol., 314, 79–90.

Chen, W.R. and **Shepherd, G.M.** (1997) *Membrane and synaptic properties of mitral cells in slices of rat olfactory bulb*. Brain Res., 745, 189–196.

Ciombor, K.J., Ennis, M. and **Shipley, M.T.** (1999) *Norepinephrine increases rat mitral cell excitatory responses to weak olfactory nerve input via alpha-1 receptors* in vitro. Neuroscience, 90, 595–606.

Czesnik, D., Nezlin, L., Rabba, J., Müller, B. and **Schild, D.** (2001) *Noradrenergic modulation of calcium currents and synaptic transmission in the olfactory bulb of* Xenopus laevis *tadpoles.* Eur. J. Neurosci., in press.

Dulac, C. and **Axel, R.** (1995) *A novel family of genes encoding putative pheromone receptors in mammals*. Cell, 83, 195–206.

Edwards, F.A., Konnerth, A., Sakmann, B. and **Takahashi, T.** (1989) *A thin slice preparation for patch clamp recordings from neurones of the mammalian central nervous system*. Pflügers Arch., 414, 600–612.

Freitag, J., Krieger, J., Strotmann, J. and **Breer, H.** (1995) *Two classes of olfactory receptors in* Xenopus laevis. Neuron, 15, 1383–1392.

Gähwiler, B.H. (1981) *Organotypic monolayer cultures of nervous tissue*. J. Neurosci. Methods, 4, 329–342.

Gähwiler, B.H. (1988) *Organotypic cultures of neural tissue*. Trends Neurosci., 11, 484–489.

Gähwiler, B.H., Capogna, M., Debanne, D., McKinney, R.A. and **Thompson, S.M.** (1997) *Organotypic slice cultures: a technique has come of age*. Trends Neurosci., 20, 471–477.

Halabisky, B., Friedman, D., Radojicic, M. and **Strowbridge, B.W.** (2000) *Calcium influx through NMDA receptors directly evokes GABA release in olfactory bulb granule cells*. J. Neurosci., 20, 5124–5134.

Heyer, B.C. and **Lux, H.D.** (1976) *Control of the delayed outward potassium currents in bursting pace-maker neurones of the snail,* Helix pomatia. J. Physiol. (Lond.), 262, 349–382.

Hille, B. (1992) Ionic Channels of Excitable Membranes. Sinauer Associates, Sunderland, MA.

Howell, B.J., Baumgardner, F.W., Bondi, K. and **Rahn, H.** (1970) *Acid-base balance in cold-blooded vertebrates as a function of body temperature*. Am. J. Physiol., 218, 600–606.

Isaacson, J.S. (1999) *Glutamate spillover mediates excitatory transmission in the rat olfactory bulb*. Neuron, 23, 377–384.

Isaacson, J.S. and **Strowbridge, B.W.** (1998) *Olfactory reciprocal synapses: dendritic signalling in the CNS*. Neuron, 20, 749–761.

Kanaki, K., Kawashima, S., Kashiwayanagi, M. and **Kurihara, K.** (1997) *Carnosine-induced inward currents in rat olfactory bulb neurons in cultured slices*. Neurosci. Lett., 231, 167–170.

Mombaerts, P. (1996) *Targeting olfaction*. Curr. Opin. Neurobiol., 6, 481–486.

Mori, K. (1987) *Membrane and synaptic properties of identified neurons in the olfactory bulb*. Prog. Neurobiol., 29, 275–320.

Nekrasova, E., Sosinskaya, A., Natochin, M., Lancet, D. and **Gat, U.** (1996) *Overexpression, solubilization and purification of rat and human olfactory receptors*. Eur. J. Biochem., 238, 28–37.

Nezlin, L.P. and **Schild, D.** (2000) *Structure of the olfactory bulb in tadpoles of* Xenopus laevis. Cell Tissue Res., 300, 21–29.

Ngai, J., Dowling, M.M., Buck, L., Axel, R. and **Chess, A.** (1993) *The family of genes encoding odorant receptors in the channel catfish*. Cell, 72, 657–666.

Nieuwkoop, P.D. and **Faber, J.** (1956) Normal Table of *Xenopus laevis* (Daudin). North Holland, Amsterdam, The Netherlands.

Raming, K., Krieger, J., Strotmann, J., Boekhoff, I., Kubick, S., Baumstark, C. and **Breer, H.** (1993) *Cloning and expression of odorant receptors*. Nature, 361, 353–356.

Scalia, F., Gallousis, G. and **Roca, S.** (1991) *A note on the organization of the amphibian olfactory bulb*. J. Comp. Neurol., 305, 435–442.

Schild, D. (1985) *A computer-controlled device for the application of odours to aquatic animals*. J. Electrophysiol. Techn., 12, 71–79.

Schild, D., Gennerich, A. and **Schultens, H.A.** (1996) *Microcontrollers as inexpensive pulse generators and parallel processors in electrophysiological experiments*. Med. Biol. Engng Comput., 34, 305–307.

Schoppa, N.E. and **Westbrook, G.L.** (1997) *Modulation of mEPSCs in olfactory bulb mitral cells by metabotropic glutamate receptors*. J. Neurophysiol., 78, 1468–1475.

Shepherd, G.M. (1972) *Synaptic organization of the mammalian olfactory bulb*. Physiol. Rev., 52, 864–917.

Trombley, P.Q. (1992) *Norepinephrine inhibits calcium currents and EPSPs via a G-protein-coupled mechanism in olfactory bulb neurons*. J. Neurosci., 12, 3992–3998.

Trombley, P.Q. and **Shepherd, G.M.** (1992) *Noradrenergic inhibition of synaptic transmission between mitral and granule cells in mammalian olfactory bulb cultures*. J. Neurosci., 12, 3985–3991.

Trombley, P.Q. and **Westbrook, G.L.** (1992) *L-AP4 inhibits calcium currents and synaptic transmission via a G-protein-coupled glutamate receptor*. J. Neurosci., 12, 2043–2050.

Wellerdieck, C., Oles, M., Pott, L., Korsching, S., Gisselmann, G. and **Hatt, H.** (1997) *Functional expression of odorant receptors of the zebrafish* Danio rerio *and of the nematode* C.elegans *in HEK293 cells*. Chem. Senses, 22, 467–476.

Weth, F., Nadler, W. and **Korsching, S.** (1996) *Nested expression domains for odorant receptors in zebrafish olfactory epithelium*. Proc. Natl Acad. Sci. USA, 93, 13321–13326.

Accepted November 27, 2000